

LOCAL CLIMATE ZONES: LESSONS FROM SINGAPORE AND POTENTIAL IMPROVEMENT WITH STREET VIEW IMAGERY

M. Ignatius¹, R. Xu², Y. Hou¹, X. Liang¹, T. Zhao³, S. Chen², N.H. Wong², F. Biljecki^{1,4,*}

¹Department of Architecture, National University of Singapore, Singapore - (m.ignatius, yujun)@nus.edu.sg, xiucheng@u.nus.edu, filip@nus.edu.sg

²Department of the Built Environment, National University of Singapore, Singapore - bdgxr@nus.edu.sg, chenshisheng@u.nus.edu, bdgwnh@nus.edu.sg

³School of Architecture and Urban Planning, Shenzhen University, China - zhaotianhong2016@email.szu.edu.cn

⁴Department of Real Estate, National University of Singapore, Singapore

Commission IV, WG IV/9

KEY WORDS: Geospatial, Urban Climate, Urban Morphology, Microclimate, Street-level Imagery

ABSTRACT:

Urban heat island (UHI) is considered a serious environmental issue in highly urbanized cities such as Singapore. To better quantify the UHI intensity, the local climate zones (LCZ) classification scheme was adopted to characterize land covers, and describe and compare their thermal performance. There are three commonly used LCZ classification approaches: manual sampling, World Urban Database and Access Portal Tools (WUDAPT) processing method using remote sensing, and geographical information system (GIS)-based method. Based on the current implementation of WUDAPT Level 0 method in the classification work in Singapore, the principal limitations are expounded. To overcome the deficiencies, street view imagery (SVI), which carries substantial urban spatial information, is regarded as a promising data source. This paper reviews the potential of SVI to better estimate certain LCZ-related properties, such as sky view factor (SVF). As it allows a detailed view on the ground objects, SVI opens up the possibility of identifying surface properties such as albedo, as well as anthropogenic heat sources. Although it is not a novel idea, there has been a lack of a comprehensive use of SVI in assisting LCZ classification from the ground up, especially in a high-density city such as Singapore. This paper overviews potential ways to incorporate SVI and identifies challenges such as coarse temporal resolution and spatial coverage constrained to drivable roads.

1. INTRODUCTION

The rise of urbanization and its impact on local thermal climate has been widely documented in scientific literature (Patra et al., 2018; Li et al., 2016; Lin et al., 2020). The urban heat island (UHI), an observation where urban air temperature is higher than in the rural area, has been reported for cities and regions worldwide. UHI effect is due to the agglomeration of diverse man-made structures that has replaced the natural landscape. However, the descriptions of urban and rural characteristics were deemed too broad, leaving vague definitions and gaps between the two extremes, where the physical and climatological characteristics in-between are not clearly defined.

To help classify the various of rural-urban regions, Stewart and Oke (2012, 2015) developed the 'local climate zones' (LCZ) classification scheme for UHI studies, to provide a framework on studying the UHI and develop a widely accepted standardization of rural-urban parameterization. LCZ comprises 17 zone types at the local scales, where each type describes a unique surface structure, land cover, construction materials and human activity. The LCZ system was initially developed to assist UHI researchers, but it has derivative uses for city planners, landscape ecologists, and global climate change investigators. LCZ has a long history of application in numerous studies, in which mostly deals with climatic mappings. Based on the recent literature review, LCZ classifications have been applied to analyze outdoor thermal comfort in various urban settings (Lau et

al., 2019; Ren et al., 2022), or evaluating regional climate and WRF (Weather Research and Forecasting) model performance (Wong et al., 2019).

Since an accurate LCZ map can contribute to a better study of urban climate issues with the concept of urban morphological details and human activity, efforts are continuously made to improve the existing LCZ classification methods. This study aims to evaluate conventional approaches and devise potential improvements. A LCZ classification case study is used to demonstrate the advantages and principle limitations of the commonly accepted method and the possible issues when adopting Geographical Information System (GIS) based method. Based on that, the potential improvement by Street View Imagery (SVI) and its feasibility are discussed. Although it is not a novel idea, there has been limited research on applying SVI to improve LCZ classifications (Demuzere et al., 2019; Wang et al., 2018a). The potential of SVI lies on its ground level information, which provides a level of detail that is not available from remote sensing data.

The current methodology and practice of LCZ classification approaches are reviewed in Section 2. A case study showing the procedure of developing a LCZ map for Singapore is presented in Section 3, while the evaluations is discussed in Section 4, which leads to the potential improvements and the feasibility study of the new method utilizing SVI in Section 5.

* Corresponding author

2. LCZ: CURRENT METHODOLOGY AND PRACTICE

2.1 LCZ Classifications

LCZ classification is based upon urban morphology, built-up, and surface cover (pervious and impervious). They are divided into 17 standard classes comprises 10 built-up types (LCZ 1 to 10) and 7 vegetation types (LCZ A to G), as illustrated in Figure 1 (Stewart and Oke, 2012). In addition, the 17 categories have 4 variable land cover properties. These classes have different microclimatic conditions, and they are associated with the air temperature, which provides a generic framework for UHI studies. After its development, the LCZ classification scheme was adopted as an international standard to classify the land cover and describe its thermal performance (Stewart and Oke, 2012; Demuzere et al., 2021; Aslam and Rana, 2022; Quan and Bansal, 2021).

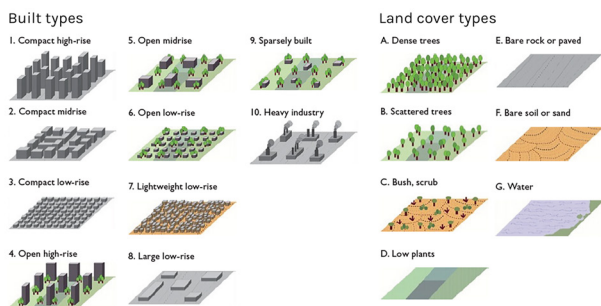


Figure 1. Local climate zones classifications, based on Stewart and Oke (2012).

2.2 Current methodologies on classifying LCZ

From previous studies, there are three known methods to perform LCZ classification according to the data sources and analytical methods: manual sampling, remote sensing (RS), and GIS.

Manual sampling requires a lot of human labor and is inefficient, which is then regarded as an unsuitable method in developing a LCZ map for a city. Remote sensing (RS) relies on object-based image analysis and machine learning techniques, which is common for continental or regional assessment, but can misclassify some built-type LCZs because of the limitations in detecting building geometry characteristics. Efforts have been exercised to standardize methods on using RS data; they have been criticized for being unjustified and unstandardized (Quan and Bansal, 2021; Geletič and Lehnert, 2016). GIS method requires a complete set of raster and vector-based planning data (Zheng et al., 2018; Lelovics et al., 2013) to conduct LCZ classification (Perera and Emmanuel, 2018; Chen et al., 2020; Rodler and Leduc, 2019; Hidalgo et al., 2019; Estacio et al., 2019; Kotharkar and Bagade, 2018).

The community ‘The World Urban Database and Access Portal Tools’ (WUDAPT) provides a fast and low-cost product of LCZ classification based on both RS images and software tools, which called WUDAPT Level 0 (Mills et al., 2015; Bechtel et al., 2019, 2015). WUDAPT Level 0 classifies the local morphologies into different LCZs and provides a 2D LCZ map in a city level. Based on its results, WUDAPT Level 1 and Level 2 gathers details on each urban elements and develops a 3D model.

The objective behind the WUDAPT initiative is to use the LCZ classification framework as the starting point for characterizing cities in a consistent manner and provide open access to data.

From the first introduction of LCZ mapping in urban environments, its implementation has bifurcated into the RS and GIS streams. The RS stream has gained popularity because of its reliance on available satellite imageries for selective cities in the world and formalized methods by WUDAPT community. GIS method does not have an internationally standardized procedure yet, and comparison studies between RS and GIS method are not conclusive about which one is more superior (Quan and Bansal, 2021).

2.3 Significance of developing a LCZ map in Singapore

As a highly dense and tropical city-state, it is an imperative for Singapore to develop an LCZ map that is better in classifying different built-types and land cover types to study urban microclimate and UHI-related issues. The study by Wong and Yu (2005) has indicated a 4°C UHI impact in Singapore, which was based on mobile measurements between the central and forest/central catchment areas. Furthermore, a qualitative and quantitative assessment on Singapore urban morphology concurs with the previous finding where the land usage will influence urban temperature (Jusuf et al., 2007). In the day time, high surface temperature is found at industrial area, while commercial area exhibits the highest at night time. This finding suggests the necessity of developing accurate islandwide LCZ classifications for Singapore.

An accurate LCZ map can describe the urban morphological information and the corresponding thermal performance at each site. Based on the results, a communication bridge can be established between urban planners and meteorologists to understand and discuss the effects of urban form on urban microclimate, which can help develop environmental friendly and functional city design.

3. RS METHOD IN CLASSIFYING LCZ: SINGAPORE CASE STUDY

In this Singapore case study, WUDAPT level 0 method using RS dataset, is utilized for classifying LCZ types. The LCZ classification workflow of WUDAPT level 0 method follows the standard processing procedures stated by WUDAPT community. The preliminary LCZ map in Singapore is shown in Figure 2.

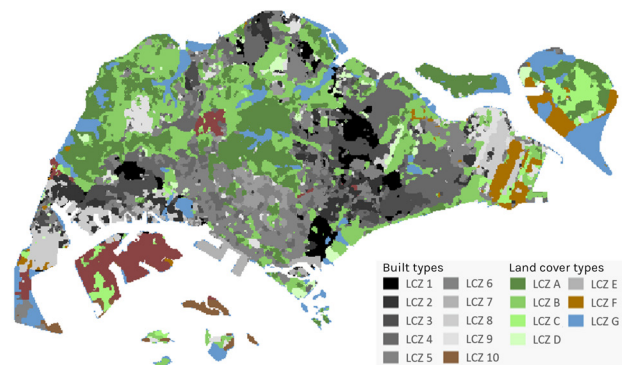


Figure 2. Preliminary LCZ classification map in Singapore.

Currently, the WUDAPT level 0 method is a satellite image-based 2-dimensional LCZ classification method that commonly accepted and utilized (Mughal et al., 2019). Landsat 8 satellite images with minimum cloud cover were selected and downloaded as input data into SAGA GIS. There were 15 LCZ samples of each classification type manually selected in Google Earth as the training groups. Then the LCZ maps with different resolutions were computed using random forest algorithm with the selected training samples. Samples in the validation group were then utilized to verify the classification accuracy. The training groups were improved until the accuracy met the requirements, by manually reselecting more suitable LCZ samples.

The following sections will briefly elaborate the current LCZ workflow and relevant dataset source limitation. Then, a proposed urban morphology quantification at ground scale is introduced to complement the deficiencies of satellite imagery.

4. EVALUATION AND LIMITATION

Two key issues arise when implementing the original LCZ framework in real-world LCZ mapping: low spatial resolution of RS data and subjective judgement for the selection of the training areas for WUDAPT level 0 method.

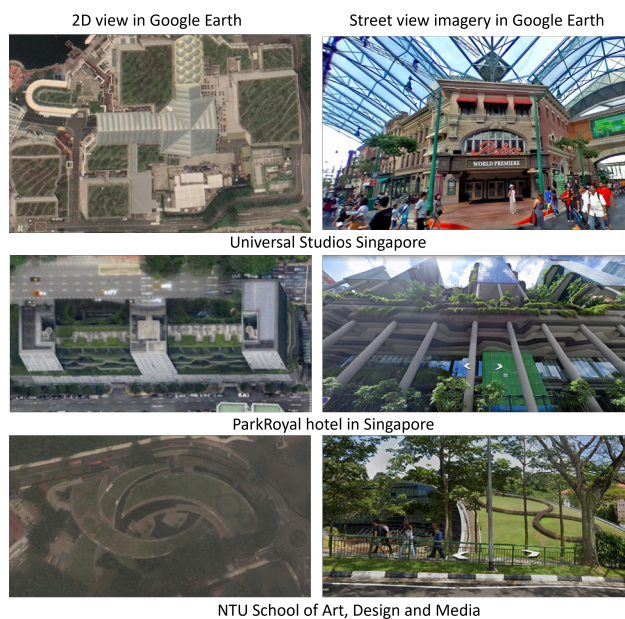


Figure 3. Examples of misleading green roofs: comparison between aerial view and street view imagery in Google Maps.

For the WUDAPT level 0 method, the identification of training areas is a difficult and time-demanding task. The LCZ scheme was not initially developed for mapping based on the spectral properties from satellite imagery. Instead, the 17 classes were differentiated according to many factors including land cover composition, urban fabric, functional use and anthropogenic factors. The geometric and surface cover properties distinguishing LCZ types (Figure 1) are often difficult to infer from satellite imagery. For example, viewers often find that building geometry is blocked by trees and vegetation, or roof gardens are misinterpreted as ground level turfing, shown in Figure 3.

Furthermore, many studies have focused on generating LCZ maps using remote sensing data, but nearly all have used tra-

ditional land use/land cover (LULC) map accuracy metrics, which penalize all map classification errors equally, to evaluate the accuracy of these maps (Johnson and Jozdani, 2019). Lipson et al. (2022) identified this top-down limitation, as there is inconsistency in data from various users and regions. They propose to use high resolution surface datasets that represent bottom-up method to obtain high fidelity 3D shapes of buildings and trees. However, such datasets are not yet available widely.

It is found difficult to develop a 3D model which describes every urban structure components, especially vegetation and ground surfaces. As for buildings, most cities do not have their complete and available appropriate geospatial datasets (Biljecki and Chow, 2022). Even with the building model, the overlapping values of the determining parameters of the LCZ classes in the method specifications may also lead to the misclassification. One can look at the LCZ table and notice that there are many overlaps in the given values of geometric properties for each class, i.e. the classes are not mutually exclusive. It means when more LCZ parameters are used for classification, it is difficult to guarantee that the values of site metadata match well with those in the standard LCZ datasheet. There is an example of the misclassification of an LCZ 5 into LCZ 10 when directly match the given values of the LCZ determining parameters, shown in Figure 4. The given parameters such as pervious surface fraction and sky view factor determine the area to be LCZ 10 while it is an obvious LCZ 5 without industrial structures.

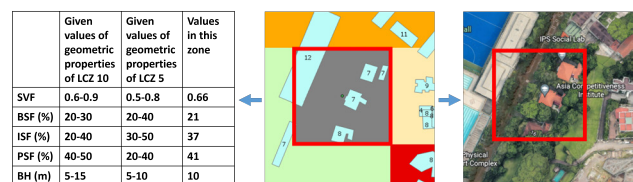


Figure 4. An example of the misclassification from LCZ 5 into LCZ 10 with the direct matching method (comparison between vector GIS data and satellite imagery in Google Earth).

Problems also arise when applying LCZ classification scheme based on the given values of geometric, surface cover, thermal, radiative, and metabolic properties for local climate zones. The urban morphology characteristics of each cities are different (Biljecki and Chow, 2022), and this is particularly the case for megacities such as Singapore, Tokyo, and Jakarta. Cities in Northern Europe tend to be more open-built, while in Asia are often more densely built. Hence, using the same classification standard, the given values of each LCZ class may not fit these high-density megacities.

Consecutively, the gaps in urban morphology characteristics between lowly and highly dense cities can lead to over or underestimated urban geometry, especially building footprints and heights, which is a common issue found in assessing high density urban areas. For example, LCZ4 is defined with 20–40% Building Surface Fraction (BSF), 30–40% Impervious Surface Fraction (ISF), and 30–40% Pervious Surface Fraction (PSF). These properties are difficult to extract from satellite imagery based on human interpretation, even from high-resolution imagery. Another issue is that LCZ4 and LCZ5 have similar surface fractions but differ in the height of roughness elements (<25 m for LCZ4 and 3–10 m for LCZ5). These two open types are difficult to label without 3D data.

Therefore, in high-density cities, such as Singapore, urban

types are difficult to be distinguished without secondary data sources. Some researchers have attempted to conduct LCZ classifications for Singapore. Mughal et al. (2019) developed Singapore LCZ by following WUDAPT level 0 methodology using Landsat 8 images and building height data. Meanwhile, Matthias et al. (2019) used cloud-computing resources of Google Earth Engine as an alternative approach of the WUDAPT method. Hence, these studies are limited on obtaining street-level information, which is essential to determine the characteristics of urban geometry and other elements. This situation is where data such as street view imagery (SVI) can provide better information.

5. POTENTIAL FOR IMPROVEMENTS

5.1 Street view imagery for LCZ classification

Street view imagery (SVI) is an emerging yet promising data source that provides rich urban spatial information, and has gained growing recognition recently owing to its usefulness, widespread availability and the increasing ease to process images in large batches (Ma et al., 2019; Mahabir et al., 2020; Biljecki and Ito, 2021). SVI data is commonly provided by commercial services such as Google Street View (GSV), and crowdsourced platforms such as Mapillary and KartaView. SVI has enabled and enhanced a wide spectrum of applications in urban-related topics including spatial data infrastructure, public health, urban greenery, transportation, mobility, perception, socioeconomics, and so on (Branson et al., 2018; Cheng et al., 2018; Zhang et al., 2019a; Pelizari et al., 2021; Li et al., 2021; Yao et al., 2021; Inoue et al., 2022; Qiu et al., 2022; Hosseini et al., 2022; Byun and Kim, 2022; Guan et al., 2022).

According to the guidelines by Stewart and Oke (2012) to use the LCZ classification system, relevant site metadata must be collected to quantify the surface properties of the thermal source area for a temperature sensor. Stewart and Oke (2012) state that such data is best collected through a field visit, but secondary sources of site metadata could be used if a site survey is not possible. SVI has been frequently used in place of site visits for environmental audit purposes, especially for studies that span across large spatial scales or focus on multiple cities which often makes site visits virtually impossible (Rundle et al., 2011; Hara et al., 2015; Yin et al., 2015; Fry et al., 2020; Ito and Biljecki, 2021).

In contrast to RS imagery, which has a top-down view, SVI provides a ground-level perspective that can be immensely valuable in estimating certain LCZ-related properties, such as sky view factor, street canyon aspect ratio, and height of roughness elements, which are difficult to obtain from optical remote sensing imagery. Further, SVI allows a closer and more detailed view on the ground objects, potentially aiding in the verification of surface properties including permeability, admittance, and albedo, as well as the identification of anthropogenic heat sources. Thus, using SVI as ancillary data for LCZ classification presents great potential in improving the classification accuracy. More specifically, we found that SVI could substantially improve the measurement or verification of all LCZ-related properties except for building surface fraction, for which remote sensing imagery would provide more accurate measurement. The next two sections (5.2 and 5.3) detail how effectively SVI could potentially enhance the determination of each LCZ-related property — either regarding their measurement or their

verification, and briefly discuss the feasibility of implementation based on existing studies. Section 5.4 describes potential ways to incorporate SVI in the LCZ classification process. We have also identified potential challenges associated with SVI as a data source in Section 5.5.

5.2 Improvement in direct measurement or estimation

Sky view factor Similar to green view factor and building view factor, sky view factor (SVF) is a dimensionless variable between 0 and 1 that represents the proportion of the area of visual hemisphere covered by sky (Liang et al., 2020), as shown in Figure 5. This indicator is commonly used to measure the canyon geometry in certain portion of a city, which has a significant impact on urban heat islands (Oke, 1981). Rather than calculating street-level SVF based on field survey, SVI opens a great opportunity to obtain the SVF measurements with fine-scale and high-coverage (Middel et al., 2018; Biljecki and Ito, 2021). This approach is examined by Wang et al. (2018a); Demuzere et al. (2019), who aggregate the spherical fractions of sky into LCZ maps to generate parameter means of SVF.

Although SVF estimation requires a complicated process from images processing to deep learning model training, there are some useful tools to mitigate the difficulty. For example, (Liang et al., 2020) introduce an easy-to-use GIS-integrated tool (GSV2SVF) to obtain SVF conveniently, which could be integrated as one of the evaluation processes of LCZ.



Figure 5. Example of original SVI panorama processed into a visual hemisphere for sky view factor calculation, together with the segmented result.



Figure 6. Comparison of the two SVF calculations by using SVI and using SAGA GIS method. The number in the brackets indicates how many SVI points were averaged to obtain the SVF value for each grid. Building footprints were obtained from OpenStreetMap.

We attempted to use some SVI data to measure SVF and compare the difference between SVI and SAGA GIS method. This data is obtained from Google through an open source script that emulates the browser (Tang and Long, 2019). The panoramic SVI are downloaded every 20 meters along the road network. The semantic segmentation model is used to extract

the pixel fraction of the sky. Specifically, we used the DeepLabV3+ model (Chen et al., 2018) trained on Cityscape dataset (Cordts et al., 2016), which includes 19 classes of labels (e.g. sky, vegetation, building, etc.). Figure 6 illustrates how SVI could potentially improve the SVF parameter. As SVI data have considered the view obstruction due to buildings, trees, and other objects, the SVF values tend to be lower compared to SAGA GIS method, which relies on building data only. As most streets in Singapore are complemented with arrays of trees, this example amplifies the significance of SVI.

Aspect ratio Similar to SVF, aspect ratio is another built environment factor that has significant impact on thermal comfort (Ali-Toudert and Mayer, 2007). However, traditional aspect ratios measurements require laborious field surveys, which inhibit large-scale investigation. While commonly used GIS-based approaches could enable large-scale investigation, they heavily rely on the availability of built environment data, such as building height and road condition information, which is often unavailable. To sense the street canyon geometry rapidly, Hu et al. (2020) developed a deep multitask learning framework to classify it into three levels. Among them, H/W-based (Level 1) divides street canyons into four categories based on canyon height (H) to canyon width (W) ratio, indicating the possibility to measure aspect ratio based on SVI instead of building height data.

Terrain roughness class Davenport et al. (2020) classified 8 terrain roughness types: sea, smooth, open, roughly open, rough, very rough, skimming, and chaotic. Each roughness type is associated with a different landscape description, such as open water, featureless landscape with little obstacles, flat land with low vegetation, open land with low buildings high crops, large farms with forest clumps, dense urban areas with low or high building-height variation, and so on (Davenport et al., 2020). These characteristics are usually difficult to determine through satellite images, but can easily be visually assessed from SVI. Although there is no existing study that focus on classifying terrain roughness using SVI, machines can potentially be trained to automatically detect the terrain roughness type around a location using SVI. Although Digital Elevation Models (DEMs) could provide information on terrain elevation, it represents the bare surface and does not provide precise observation at a local scale, which could make it difficult to identify objects that can influence the classification such as low vegetation and crops. SVI could thus be used to provide more precise information.

5.3 Improvement in verification

Impervious and pervious surface fractions Under the land-cover category, impervious and pervious surface fractions are the main contributors to land surface temperature that could further perpetuate urban heat issues. However, due to the obscuration of vegetation and man-made structures, the traditional approach relies heavily on manual measurements or low precision estimates from remote sensing (Imhoff et al., 2010). Thanks to various training data created according to different research purposes, SVI enable researchers to measure different surface fraction according to the proportions of certain elements (Figure 7). For example, Middel et al. (2019) aggregate 33 semantic classes from SIFT Flow dataset into four surface types, including impervious surfaces and pervious surfaces. To be specific, impervious surfaces include urban features such as bridges, crosswalks, roads, sidewalks, roofs, etc., while the index of pervious

surface is generated from classes such as fields, grass, rivers and sea. This method is further examined by Zhang et al. (2019b), who compare the surfaces fraction generated from spherical and planar aspects and verify street view can provide better estimation for land surface temperature.

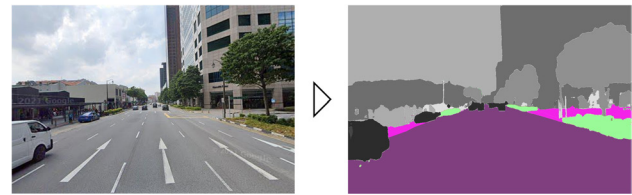


Figure 7. Example of impervious and pervious features (purple–road, pink–sidewalk, green–grass) extracted based on model trained on Cityscape dataset (Cordts et al., 2016).

Height of roughness elements According to physical properties of LCZs, the height of roughness elements is considered from two aspects: building heights and tree/plant heights. These two indicators are usually unavailable at city scale and largely rely on field surveys. To address this obstacle, Wang et al. (2018b) apply scale-independent, fixed-sized street objects to recalibrate the heights of vegetation based on SVI. Similarly, Yuan and Cheriyyadat (2016) and Zhao et al. (2019) integrate building footprints and SVI to estimate building heights at small scale. Although these methods provide opportunities to obtain the height of buildings/vegetation based on SVI, the elements within areas that are vehicle-inaccessible, are difficult to measure. To generally describe height conditions of an area, alternative datasets, such as remote sensing images, synthetic aperture radar (SAR) images and aerial LiDAR data, could have better performance.

Surface admittance, surface albedo, and anthropogenic heat flux Although no existing studies have specifically focused on deriving a method to automatically extract, from SVI, climate-related building surface properties such as admittance and albedo, SVI undeniably provides a more detailed view that would make it much easier to identify building surface materials, which could then be used to verify surface admittance and albedo data obtained from other sources. It is also easy to visually assess the land use type around an area using SVI (e.g. residential, commercial, industrial, etc.) which could help verify the expected range of anthropogenic heat flux in that area given the observed land use type. Automated approach using computer vision has also been devised. For example, Kang et al. (2018) proposed a deep-learning approach to classify the functionality of individual buildings, into categories including industrial, office building, house, retail, etc. This approach could provide insights for verifying anthropogenic heat flux data, automatically over a large spatial scale. Yang and Wang (2021) and Arjunan et al. (2021) used computer vision to automatically detect external air-conditioner units, which could also provide information on anthropogenic heat sources.

5.4 Potential ways to incorporate SVI

Sample locations within areas of classification interest could be randomly selected, and street view panoramas at these locations could be obtained from a SVI service via their API. Then, LCZ-related properties such as aspect ratio and terrain roughness class could be labeled, and properties including impervious or pervious surface fraction, height of roughness elements, surface admittance albedo and anthropogenic heat flux could be

verified, by a panel of experts, or by a crowdsourced group of trained workers (e.g. through Amazon Mechanical Turk), similar to the crowdsourcing methods adopted in various studies (Hara et al., 2012, 2015; Kruse et al., 2021). Sky view factor, on the other hand, shows the highest potential to be automatically extracted from SVI, which is affirmed by an increasing number of studies. Information extracted from these sample points could be integrated with other datasets to support the classification of LCZs.

SVI could also be used to identify places suitable for placing temperature sensors. According to the guidelines by Stewart and Oke (2012), a sensor should ideally sample from a single LCZ, and the land cover and exposure characteristics of the location should be representative of the designated LCZ (e.g. sheltered street canyon with paved ground for LCZs 1-3). SVI allows us to remotely view the detailed setting of an urban environment. Thus, if sufficiently recent, SVI could also be used in place of field visits to search for suitable places for placing the sensor.

5.5 Potential challenges

Unlike satellite imagery which has consistent and global coverage, the spatial coverage of SVI is not complete and can be inconsistent across different years (i.e. a location covered by SVI in one year may not be covered in another year). This limitation means that it could be difficult to use SVI to improve LCZ classification for areas with low SVI availability, and it could be difficult to ensure the same effectiveness of SVI on LCZ classification for a multi-year study. Further, SVI is mostly collected along roads. Although it is useful for estimating properties such as sky view factor and street canyon aspect ratio, information for areas beyond the streets may be difficult to infer. Image quality issues, such as blurriness, which could be heterogeneously present in a SVI dataset, could also make observation difficult. Very tall buildings near the camera could exceed the image frame, making it difficult to estimate canyon aspect ratio or building height. Certain ephemeral characteristics of land cover (e.g. snow cover, dry or wet ground, bare trees) could be hard to detect using SVI, as SVI may not be updated in a timely manner. It is thus important to consider both spatial and temporal characteristics of SVI data, when designing the methodology to incorporate SVI to classify LCZs, especially for multi-year studies.

6. CONCLUSION

This study discussed the advantages and limitations of manual sampling, GIS and remote sensing for LCZ classification, an instrumental concept in climate studies. Based on the current implementation of WUDAPT Level 0 method in the classification work in Singapore, low spatial resolution of RS data and subjective judgment for the selection of the training areas can result in unsatisfactory accuracy for WUDAPT Level 0 method, requiring research on alternative approaches.

In addition, issues in the commonly used GIS-based classification method can be found due to lack of data and unclear method specifications. Problems also arise when applying the same LCZ classification scheme based on the given values of geometric, surface cover, thermal, radiative, and metabolic properties to determine the LCZ types in cities with different urban morphology characteristics, such as densely built Asian megacities and open-built cities in Northern Europe.

To improve LCZ classification, SVI, which conveys substantial urban spatial information, provided by commercial services such as Google Street View (GSV) and crowdsourced platforms such as Mapillary and KartaView, is regarded as a promising data source. It has been used in LCZ studies, but rarely and to a limited extent (to estimate the sky view factor) and in this paper we argue that its potential goes further than that: it can be utilized to also better estimate certain LCZ-related properties such as street canyon aspect ratio and height of roughness elements.

In particular, accurate SVF plays an important role in classifying LCZ types. It cannot be simulated by a GIS-driven model without precise vegetation information, or remote sensing imagery with a top-down view, but can be easily obtained from SVI with a ground-level perspective. This has been illustrated with the preliminary study presented, which reinforces the case of using ground level data to determine the SVF. Furthermore, SVI allows a detailed view on the ground objects, opening up the possibility of identifying surface properties including permeability, admittance, and albedo, as well as anthropogenic heat sources, while it is difficult to be captured by both GIS-based method and WUDAPT Level 0 method.

The lesson from Singapore case study indicates that LCZ classification process at high-density urban areas, where tall buildings and trees are prominent, requires higher fidelity data sets at the ground level. This preliminary feasibility study indicates the potential ways to incorporate SVI and the potential challenges. Further studies will be focused on the implementation. We will conduct experiments to evaluate the accuracy of the LCZ classification method relying on SVI, and the integration between SVI and the commonly used GIS-based and WUDAPT Level 0 methods.

ACKNOWLEDGEMENTS

The authors gratefully acknowledge the LCZ classification results in Singapore by Dr. Tong Shanshan, Dr. Fan Ke, Dr. Zhang Wen, and Mr. Wu Xinyi. This research is part of the projects (i) Development of Thermal aerodynamic Models for Local Climate Zones (DTMLCZ)' and (ii) Smart Cities and Urban Analytics, which were supported by the National Research Foundation Singapore (NRF2018NRF-NSFC003ES-012 and R-295-000-194-281); (iii) Large-scale 3D Geospatial Data for Urban Analytics, which is supported by the National University of Singapore under the Start Up Grant R-295-000-171-133; and (iv) Multi-scale Digital Twins for the Urban Environment: From Heartbeats to Cities, which is supported by the Singapore Ministry of Education Academic Research Fund Tier 1.

References

- Ali-Toudert, F., Mayer, H., 2007. Effects of asymmetry, galleries, overhanging facades and vegetation on thermal comfort in urban street canyons. *Solar energy*, 81(6), 742–754.
- Arjunan, P., Dobler, G., Lee, K., Miller, C., Biljecki, F., Poolla, K., 2021. Operational characteristics of residential air conditioners with temporally granular remote thermographic imaging. *BUILDsys '21: Proceedings of the 8th ACM International Conference on Systems for Energy-Efficient Buildings, Cities, and Transportation*, 184–187.
- Aslam, A., Rana, I. A., 2022. The use of local climate zones in the urban environment: A systematic review of data sources, methods, and themes. *Urban Climate*, 42, 101120.

- Bechtel, B., Alexander, P. J., Beck, C., Böhner, J., Brousse, O., Ching, J., Demuzere, M., Fonte, C., Gál, T., Hidalgo, J. et al., 2019. Generating WUDAPT Level 0 data—Current status of production and evaluation. *Urban climate*, 27, 24–45.
- Bechtel, B., Alexander, P. J., Böhner, J., Ching, J., Conrad, O., Feddema, J., Mills, G., See, L., Stewart, I., 2015. Mapping local climate zones for a worldwide database of the form and function of cities. *ISPRS International Journal of Geo-Information*, 4(1), 199–219.
- Biljecki, F., Chow, Y. S., 2022. Global Building Morphology Indicators. *Computers, Environment and Urban Systems*, 95, 101809.
- Biljecki, F., Ito, K., 2021. Street view imagery in urban analytics and GIS: A review. *Landscape and Urban Planning*, 215, 104217.
- Branson, S., Wegner, J. D., Hall, D., Lang, N., Schindler, K., Perona, P., 2018. From Google Maps to a fine-grained catalog of street trees. *ISPRS Journal of Photogrammetry and Remote Sensing*, 135, 13–30.
- Byun, G., Kim, Y., 2022. A street-view-based method to detect urban growth and decline: A case study of Midtown in Detroit, Michigan, USA. *PLoS ONE*, 17(2), e0263775.
- Chen, L.-C., Zhu, Y., Papandreou, G., Schroff, F., Adam, H., 2018. Encoder-decoder with atrous separable convolution for semantic image segmentation. *Proceedings of the European conference on computer vision (ECCV)*, 801–818.
- Chen, Y., Zheng, B., Hu, Y., 2020. Mapping Local Climate Zones Using ArcGIS-Based Method and Exploring Land Surface Temperature Characteristics in Chenzhou, China. *Sustainability*, 12(7), 2974.
- Cheng, L., Yuan, Y., Xia, N., Chen, S., Chen, Y., Yang, K., Ma, L., Li, M., 2018. Crowd-sourced pictures geo-localization method based on street view images and 3D reconstruction. *ISPRS Journal of Photogrammetry and Remote Sensing*, 141, 72–85.
- Cordts, M., Omran, M., Ramos, S., Rehfeld, T., Enzweiler, M., Benenson, R., Franke, U., Roth, S., Schiele, B., 2016. The cityscapes dataset for semantic urban scene understanding. *Proceedings of the IEEE conference on computer vision and pattern recognition*, 3213–3223.
- Davenport, A., Grimmond, S., Oke, T., Wieringa, J., 2020. Estimating the roughness of cities and sheltered country. *12th Conference on Applied Climatology, Asheville, NC, Amer. Meteor. Soc.*, 96-99.
- Demuzere, M., Bechtel, B., Middel, A., Mills, G., 2019. Mapping Europe into local climate zones. *PLoS one*, 14(4), e0214474.
- Demuzere, M., Kittner, J., Bechtel, B., 2021. LCZ Generator: A Web Application to Create Local Climate Zone Maps. *Frontiers in Environmental Science*, 9.
- Estacio, I., Babaan, J., Pecson, N., Blanco, A., Escoto, J., Alcantara, C., 2019. GIS-based mapping of local climate zones using fuzzy logic and cellular automata. *International Archives of the Photogrammetry, Remote Sensing & Spatial Information Sciences*.
- Fry, D., Mooney, S. J., Rodríguez, D. A., Caiaffa, W. T., Lovasi, G. S., 2020. Assessing Google Street View Image Availability in Latin American Cities. *Journal of Urban Health*, 97(4), 552–560.
- Geletič, J., Lehnert, M., 2016. GIS-based delineation of local climate zones: The case of medium-sized Central European cities. *Moravian Geographical Reports*, 24(3), 2–12.
- Guan, F., Fang, Z., Wang, L., Zhang, X., Zhong, H., Huang, H., 2022. Modelling people's perceived scene complexity of real-world environments using street-view panoramas and open geodata. *ISPRS Journal of Photogrammetry and Remote Sensing*, 186, 315–331.
- Hara, K., Azenkot, S., Campbell, M., Bennett, C. L., Le, V., Pannella, S., Moore, R., Minckler, K., Ng, R. H., Froehlich, J. E., 2015. Improving Public Transit Accessibility for Blind Riders by Crowdsourcing Bus Stop Landmark Locations with Google Street View: An Extended Analysis. *ACM Transactions on Accessible Computing*, 6(2), 5:1–5:23.
- Hara, K., Le, V., Froehlich, J., 2012. A feasibility study of crowdsourcing and google street view to determine sidewalk accessibility. *Proceedings of the 14th International ACM SIGACCESS Conference on Computers and Accessibility*, ASSETS '12, Association for Computing Machinery, New York, NY, USA, 273–274.
- Hidalgo, J., Dumas, G., Masson, V., Petit, G., Bechtel, B., Bocher, E., Foley, M., Schoetter, R., Mills, G., 2019. Comparison between local climate zones maps derived from administrative datasets and satellite observations. *Urban Climate*, 27, 64–89.
- Hosseini, M., Miranda, F., Lin, J., Silva, C. T., 2022. Citysurfaces: City-scale semantic segmentation of sidewalk materials. *Sustainable Cities and Society*, 79, 103630.
- Hu, C.-B., Zhang, F., Gong, F.-Y., Ratti, C., Li, X., 2020. Classification and mapping of urban canyon geometry using Google Street View images and deep multitask learning. *Building and Environment*, 167, 106424.
- Imhoff, M. L., Zhang, P., Wolfe, R. E., Bounoua, L., 2010. Remote sensing of the urban heat island effect across biomes in the continental USA. *Remote sensing of environment*, 114(3), 504–513.
- Inoue, T., Manabe, R., Murayama, A., Koizumi, H., 2022. Landscape value in urban neighborhoods: A pilot analysis using street-level images. *Landscape and Urban Planning*, 221, 104357.
- Ito, K., Biljecki, F., 2021. Assessing Bikeability with Street View Imagery and Computer Vision. *Transportation Research Part C: Emerging Technologies*, 132, 103371.
- Johnson, B. A., Jozdani, S. E., 2019. Local Climate Zone (LCZ) Map Accuracy Assessments Should Account for Land Cover Physical Characteristics that Affect the Local Thermal Environment. *Remote Sensing*, 11(20), 2420.
- Jusuf, S. K., Wong, N. H., Hagen, E., Anggoro, R., Hong, Y., 2007. The influence of land use on the urban heat island in Singapore. *Habitat International*, 31(2), 232-242.
- Kang, J., Körner, M., Wang, Y., Taubenböck, H., Zhu, X. X., 2018. Building instance classification using street view images. *ISPRS Journal of Photogrammetry and Remote Sensing*, 145, 44–59.
- Kotharkar, R., Bagade, A., 2018. Local Climate Zone classification for Indian cities: A case study of Nagpur. *Urban climate*, 24, 369–392.
- Kruse, J., Kang, Y., Liu, Y.-N., Zhang, F., Gao, S., 2021. Places for Play: Understanding Human Perception of Playability in Cities Using Street View Images and Deep Learning. *Computers, Environment and Urban Systems*, 90, 101693.
- Lau, K. K.-L., Chung, S. C., Ren, C., 2019. Outdoor thermal comfort in different urban settings of sub-tropical high-density cities: An approach of adopting local climate zone (LCZ) classification. *Building and Environment*, 154, 227-238.
- Lelovics, E., Gál, T., Unger, J., 2013. Mapping local climate zones with a vector-based GIS method. *Aerul si Apa. Componente ale Mediului*, 423.
- Li, S., Ma, S., Tong, D., Jia, Z., Li, P., Long, Y., 2021. Associations between the quality of street space and the attributes of the built environment using large volumes of street view pictures. *Environment and Planning B: Urban Analytics and City Science*, 239980832110563.
- Li, X.-X., Koh, T.-Y., Panda, J., Norford, L. K., 2016. Impact of urbanization patterns on the local climate of a tropical city, Singapore: An ensemble study. *Journal of Geophysical Research: Atmospheres*, 121(9), 4386–4403.
- Liang, J., Gong, J., Zhang, J., Li, Y., Wu, D., Zhang, G., 2020. GSV2SVF—an interactive GIS tool for sky, tree and building view factor estimation from street view photographs. *Building and Environment*, 168, 106475.

- Lin, L., Gao, T., Luo, M., Ge, E., Yang, Y., Liu, Z., Zhao, Y., Ning, G., 2020. Contribution of urbanization to the changes in extreme climate events in urban agglomerations across China. *Science of the total environment*, 744, 140264.
- Lipson, M. J., Nazarian, N., Hart, M. A., Nice, K. A., Conroy, B., 2022. A Transformation in City-Descriptive Input Data for Urban Climate Models. *Frontiers in Environmental Science*, 10.
- Ma, D., Fan, H., Li, W., Ding, X., 2019. The State of Mapillary: An Exploratory Analysis. *ISPRS International Journal of Geo-Information*, 9(1), 10.
- Mahabir, R., Schuchard, R., Crooks, A., Croitoru, A., Stefanidis, A., 2020. Crowdsourcing Street View Imagery: A Comparison of Mapillary and OpenStreetCam. *ISPRS International Journal of Geo-Information*, 9(6), 341.
- Matthias, D., Benjamin, B., Gerald, M., 2019. Global transferability of local climate zone models. *Urban Climate*, 27, 46-63.
- Middel, A., Lukaszczuk, J., Maciejewski, R., Demuzere, M., Roth, M., 2018. Sky View Factor footprints for urban climate modeling. *Urban climate*, 25, 120–134.
- Middel, A., Lukaszczuk, J., Zakrzewski, S., Arnold, M., Maciejewski, R., 2019. Urban form and composition of street canyons: A human-centric big data and deep learning approach. *Landscape and Urban Planning*, 183, 122–132.
- Mills, G., Ching, J., See, L., Bechtel, B., Foley, M., 2015. An introduction to the wudapt project. *Proceedings of the 9th International Conference on Urban Climate, Toulouse, France*, 20–24.
- Mughal, M. O., Li, X.-X., Yin, T., Martilli, A., Brousse, O., Dissegna, M. A., Norford, L. K., 2019. High-Resolution, Multilayer Modeling of Singapore's Urban Climate Incorporating Local Climate Zones. *Journal of Geophysical Research: Atmospheres*, 124(14), 7764-7785.
- Oke, T. R., 1981. Canyon geometry and the nocturnal urban heat island: comparison of scale model and field observations. *Journal of climatology*, 1(3), 237–254.
- Patra, S., Sahoo, S., Mishra, P., Mahapatra, S. C., 2018. Impacts of urbanization on land use/cover changes and its probable implications on local climate and groundwater level. *Journal of urban management*, 7(2), 70–84.
- Pelizari, P. A., Geiß, C., Aguirre, P., María, H. S., Peña, Y. M., Taubenböck, H., 2021. Automated building characterization for seismic risk assessment using street-level imagery and deep learning. *ISPRS Journal of Photogrammetry and Remote Sensing*, 180, 370–386.
- Perera, N., Emmanuel, R., 2018. A “Local Climate Zone” based approach to urban planning in Colombo, Sri Lanka. *Urban Climate*, 23, 188–203.
- Qiu, W., Zhang, Z., Liu, X., Li, W., Li, X., Xu, X., Huang, X., 2022. Subjective or objective measures of street environment, which are more effective in explaining housing prices? *Landscape and Urban Planning*, 221, 104358.
- Quan, S. J., Bansal, P., 2021. A systematic review of GIS-based local climate zone mapping studies. *Building and Environment*, 196, 107791.
- Ren, J., Yang, J., Zhang, Y., Xiao, X., Xia, J. C., Li, X., Wang, S., 2022. Exploring thermal comfort of urban buildings based on local climate zones. *Journal of Cleaner Production*, 340, 130744.
- Rodler, A., Leduc, T., 2019. Local climate zone approach on local and micro scales: Dividing the urban open space. *Urban Climate*, 28, 100457.
- Rundle, A. G., Bader, M. D., Richards, C. A., Neckerman, K. M., Teitler, J. O., 2011. Using Google Street View to Audit Neighborhood Environments. *American journal of preventive medicine*, 40(1), 94–100.
- Stewart, I. D., Oke, T. R., 2012. Local climate zones for urban temperature studies. *Bulletin of the American Meteorological Society*, 93(12), 1879–1900.
- Stewart, I. D., Oke, T. R., 2015. *Local climate zones and urban climatic mapping*. 1 edn, Routledge, London, book section 29, 528.
- Tang, J., Long, Y., 2019. Measuring visual quality of street space and its temporal variation: Methodology and its application in the Hutong area in Beijing. *Landscape and Urban Planning*, 191, 103436.
- Wang, C., Middel, A., Myint, S. W., Kaplan, S., Brazel, A. J., Lukaszczuk, J., 2018a. Assessing local climate zones in arid cities: The case of Phoenix, Arizona and Las Vegas, Nevada. *ISPRS Journal of Photogrammetry and Remote Sensing*, 141, 59–71.
- Wang, W., Xiao, L., Zhang, J., Yang, Y., Tian, P., Wang, H., He, X., 2018b. Potential of Internet street-view images for measuring tree sizes in roadside forests. *Urban Forestry & Urban Greening*, 35, 211–220.
- Wong, M. M. F., Fung, J. C. H., Ching, J., Yeung, P. P. S., Tse, J. W. P., Ren, C., Wang, R., Cai, M., 2019. Evaluation of uWRF performance and modeling guidance based on WUDAPT and NUDAPT UCP datasets for Hong Kong. *Urban Climate*, 28, 100460.
- Wong, N. H., Yu, C., 2005. Study of green areas and urban heat island in a tropical city. *Habitat International*, 29(3), 547-558.
- Yang, F., Wang, M., 2021. Deep Learning-Based Method for Detection of External Air Conditioner Units from Street View Images. *Remote Sensing*, 13(18), 3691.
- Yao, Y., Zhang, J., Qian, C., Wang, Y., Ren, S., Yuan, Z., Guan, Q., 2021. Delineating urban job-housing patterns at a parcel scale with street view imagery. *International Journal of Geographical Information Science*, 35(10), 1–24.
- Yin, L., Cheng, Q., Wang, Z., Shao, Z., 2015. ‘Big Data’ for Pedestrian Volume: Exploring the Use of Google Street View Images for Pedestrian Counts. *Applied Geography*, 63, 337–345.
- Yuan, J., Cheriyyadat, A. M., 2016. Combining maps and street level images for building height and facade estimation. *Proceedings of the 2nd ACM SIGSPATIAL Workshop on Smart Cities and Urban Analytics*, 1–8.
- Zhang, F., Wu, L., Zhu, D., Liu, Y., 2019a. Social sensing from street-level imagery: A case study in learning spatio-temporal urban mobility patterns. *ISPRS Journal of Photogrammetry and Remote Sensing*, 153, 48–58.
- Zhang, Y., Middel, A., Turner, B., 2019b. Evaluating the effect of 3D urban form on neighborhood land surface temperature using Google Street View and geographically weighted regression. *Landscape Ecology*, 34(3), 681–697.
- Zhao, Y., Qi, J., Zhang, R., 2019. Cbhe: Corner-based building height estimation for complex street scene images. *The World Wide Web Conference*, 2436–2447.
- Zheng, Y., Ren, C., Xu, Y., Wang, R., Ho, J., Lau, K., Ng, E., 2018. GIS-based mapping of Local Climate Zone in the high-density city of Hong Kong. *Urban climate*, 24, 419–448.